

TORUS-BREAKDOWN NEAR A BYKOV ATTRACTOR: A CASE STUDY

LUÍSA CASTRO

CENTER FOR HEALTH TECHNOLOGY AND SERVICES RESEARCH - CINTESIS,
UNIVERSITY OF PORTO,
RUA DR. PLÁCIDO DA COSTA, 4200-450 PORTO, PORTUGAL

AND

ALEXANDRE A. P. RODRIGUES

CENTRO DE MATEMÁTICA DA UNIVERSIDADE DO PORTO
AND FACULDADE DE CIÊNCIAS DA UNIVERSIDADE DO PORTO
RUA DO CAMPO ALEGRE 687, 4169-007 PORTO, PORTUGAL

ABSTRACT. There are few explicit examples in the literature of vector fields exhibiting complex dynamics that may be proved analytically. This paper reports numerical experiments performed for an explicit two-parameter family of vector fields unfolding an attracting heteroclinic network, linking two saddle-foci with $(\mathbb{SO}(2) \oplus \mathbb{Z}_2)$ -symmetry. The vector field is the restriction to \mathbb{S}^3 of a polynomial vector field in \mathbb{R}^4 . We investigate global bifurcations due to symmetry-breaking and we detect strange attractors via a phenomenon called *Torus-Breakdown theory*. We explain how an attracting torus gets destroyed by following the changes in the invariant manifolds of the saddle-foci.

Although a complete understanding of the corresponding bifurcation diagram and the mechanisms underlying the dynamical changes is still out of reach, using a combination of theoretical tools and computer simulations, we have uncovered some complex patterns for the symmetric family under analysis. This also suggests a route to obtain rotational horseshoes; additionally, we give an attempt to elucidate some of the bifurcations involved in an Arnold wedge.

We explicitly construct a two-parameter family of polynomial differential equations, in which each parameter controls a type of symmetry-breaking. We discuss global bifurcations that occur as the two parameters vary, namely the emergence of strange attractors. This route to chaos has been a recurrent concern on nonlinear dynamics during the last decades.

We use a systematic method to construct examples of vector fields with simple forms that make their dynamical properties amenable to analytic proof. The method consists of using symmetry to obtain “gradient-like dynamics” and then choosing special symmetry-breaking nonlinear terms with a simple form that preserve the required properties and introduce some desired behaviour.

2010 *Mathematics Subject Classification.* 34C28; 34C37; 37D05; 37D45; 37G35

Keywords: Global bifurcations, Bykov attractor; Heteroclinic network; Torus-Breakdown Theory; Strange attractors, Symmetry-breaking.

For this class of examples, we show the existence of many complicated dynamical objects and the complex transition between different types of dynamics, ranging from an attracting torus to Hénon-like strange attractors, as a consequence of the *Torus-Breakdown theory*. Different symmetries are broken gradually and independently; different phenomena are associated to the inclusion of different symmetry-breaking terms.

1. INTRODUCTION

A compact attractor is said *strange* if it contains a dense orbit with at least one positive Lyapunov exponent. The rigorous proof of the strange character of an invariant set is a great challenge and the proof of their prevalence in the space of parameters (persistence with respect to the Lebesgue measure) is a very involving task.

In the present paper, illustrating theoretical results of [31], we construct a two-parameter symmetric family of polynomial differential equations inspired in [5], and we show some evidences for the existence of strange attractors in its unfolding. Using the *maximal Lyapunov exponent* along an orbit, we explore numerically a mechanism to obtain strange attractors in the unfolding of an equivariant vector field. The abundance of strange attractors will be a consequence of the *Torus-Breakdown Theory* developed in [1, 3, 4, 10].

1.1. Lyapunov exponents. A *Lyapunov exponent* associated to a solution of a differential equation is an average exponential rate of divergence or convergence of nearby trajectories in the phase space. As they measure the rate at which the dynamics creates or destroys information, the Lyapunov exponents equal in number the dimension of the phase space and allow us to distinguish between chaos and regular dynamics (stable periodicity).

A positive exponent reflects the existence of a direction in which the system experiences the repeated stretching and folding that mixes nearby states on the attractor. Thus, the long-term behavior of an initial condition with a positive Lyapunov exponent cannot be predicted, and this is one of the most common features of chaos. This is the key idea behind several numerical experiments with chaotic dynamical systems. Since nearby solutions may correspond to numerical almost identical states, the presence of exponential orbital divergence implies that trajectories whose initial conditions are hard to distinguish will soon depart, and most likely behave afterwards quite differently.

The study of the number of positive Lyapunov exponents along well chosen orbits¹ motivates one of the most powerful computational techniques available to build a reliable approximation of a bifurcation diagram.

1.2. This article. We start with a detailed study of the two-parameter polynomial differential equation: equilibria, symmetries, flow-invariant sets, relative positions of the invariant manifolds, heteroclinic connections, Lyapunov stability. Then, we perform several illustrative computer experiments using Matlab (R219b, Mathworks, Natick, MA, USA) for this family of vector fields. The periodic or chaotic nature of solutions could only be determined on a case-by-case examination by fixing parameters and investigating the dynamics for well chosen initial conditions. Additional care was needed while interpreting the numerical integration of these flows since, for some parameters, they exhibit *quasi-stochastic attractors* [2] and these are prone to rounding errors that may ruin the simulations.

¹In general, these well chosen orbits correspond to the unstable manifolds of invariant saddles.

This article is organised as follows. In Section 2, based on [5, 31] we revisit the setting of symmetric Bykov attractors and the main theoretical results that state the existence of strange attractors. In Section 3, we exhibit an explicit two-parameter family of equivariant vector fields that will be the object of consideration throughout the paper. The construction of the vector field is amenable to the analytic proof of the features that guarantee complex behaviour. We illustrate dynamical phenomena in that example (when parameters vary) going from an attracting torus to horseshoes. In Section 4, we describe the expected theory about the emergence of strange attractors from an attracting torus breaking. We will see that the numerics of this section agree perfectly well with the existing theory on the topic. Finally, in Section 5, we discuss the results relating them with others in the literature. For reader's convenience, we have compiled at the end of the manuscript a list of definitions in a short glossary.

2. THE THEORY – AN OVERVIEW

Our object of study is the dynamics around an attracting heteroclinic network for which we give a rigorous description here. For each subset $M \subset \mathbb{S}^3$, we denote by \overline{M} its topological closure in \mathbb{S}^3 . In order not to interrupt the flow of ideas, we refer to Appendix A for the technical definitions of some of the terms.

2.1. The organising center. For $\varepsilon > 0$ small enough, consider the two-parameter family of C^3 -smooth differential equations

$$\dot{x} = f_{(A,\lambda)}(x) \quad x \in \mathbb{S}^3 \quad A, \lambda \in [0, \varepsilon] \quad (2.1)$$

and denote by $\varphi_{(A,\lambda)}(t, x)$, $t \in \mathbb{R}$, the associated flow, satisfying the following hypotheses for $A = 0$ and $\lambda = 0$:

(P1) There are two hyperbolic equilibria, say O_1 and O_2 .

(P2) The spectrum of Df_X is:

(P2a) E_1 and $-C_1 \pm \omega_1 i$ where $C_1 > E_1$, $\omega_1 > 0$, for $X = O_1$;

(P2b) $-C_2$ and $E_2 \pm \omega_2 i$ where $C_2 > E_2$, $\omega_2 > 0$, for $X = O_2$.

Thus the equilibrium O_1 possesses a 2-dimensional stable and 1-dimensional unstable manifold and the equilibrium O_2 possesses a 1-dimensional stable and 2-dimensional unstable manifold. We assume that:

(P3) The sets $\overline{W^u(O_2)}$ and $\overline{W^s(O_1)}$ coincide and $\overline{W^u(O_2) \cap W^s(O_1)}$ consists of a two-sphere (also called the $2D$ -connection) containing O_1 and O_2 .

and

(P4) There are two trajectories, say γ_1, γ_2 , contained in $W^u(O_1) \cap W^s(O_2)$, one in each connected component of $\mathbb{S}^3 \setminus \overline{W^u(O_2)}$ (called the $1D$ -connections).

The two equilibria O_1 and O_2 , the two-dimensional heteroclinic connection from O_2 to O_1 referred in **(P3)** and the two trajectories listed in **(P4)** build a heteroclinic network we will denote hereafter by Γ . This set has a *global attracting* character, this is why it will be called by *Bykov attractor*; terminology and details in (A.1) and (A.2). In particular, we may find an open neighborhood \mathcal{U} of the heteroclinic network Γ having its boundary transverse to the flow associated to the vector field $f_{(0,0)}$ and such that every solution starting in \mathcal{U} remains in it for all positive time and is forward asymptotic to Γ (Lemma 2.1 of [31]).

There are two possibilities for the geometry of the flow around each saddle-focus of the network Γ , depending on the direction the solutions turn around [$O_1 \rightarrow O_2$]. We assume that:

(P5) The saddle-foci O_1 and O_2 have the same chirality (details in (A.3)).

For $r \geq 3$, denote by $\mathfrak{X}^r(\mathbb{S}^3)$, the set of two-parameter families of C^r -vector fields on \mathbb{S}^3 endowed with the C^r -Whitney topology, satisfying Properties **(P1)**–**(P5)**.

2.2. Perturbing terms. With respect to the effect of the two parameters A and λ on the dynamics, we assume that:

(P6) For all $A > \lambda \geq 0$, the two trajectories within $W^u(O_1) \cap W^s(O_2)$ persist.

(P7) For all $A > \lambda \geq 0$, the two-dimensional manifolds $W^u(O_2)$ and $W^s(O_1)$ do not intersect.

Rodrigues [31] created a model assuming an extra technical hypothesis (for $A > \lambda \geq 0$):

(P8) The transitions along the connections [$O_1 \rightarrow O_2$] and [$O_2 \rightarrow O_1$] are given, in local coordinates, by the Identity map and, up to high order terms, by

$$(x, y) \mapsto (x, y + A + \lambda\Phi(x))$$

respectively, where $\Phi : \mathbb{S}^1 \rightarrow \mathbb{S}^1$ is a Morse smooth function with at least two non-degenerate critical points ($\mathbb{S}^1 = \mathbb{R} \pmod{2\pi}$).

Hypothesis **(P8)** is natural when we consider the *Melnikov integral* [15] applied to a differential equation of the type (2.1). The distance between $W_{\text{loc}}^u(O_2)$ and $W_{\text{loc}}^s(O_1)$ in a given cross section to Γ may depend on a variable x and it decomposes as

$$Mel(x) = Mel_1 + \lambda Mel_2(x)$$

where $Mel_1 \equiv A$ gives the averaged distance between $W_{\text{loc}}^u(O_2)$ and $W_{\text{loc}}^s(O_1)$ in the given cross section and $Mel_2 \equiv \Phi$ describes fluctuations of the unstable manifold of O_2 . To simplify the notation, in what follows we will sometimes drop the subscript (A, λ) , unless there is some risk of misunderstanding.

2.3. Notation. From now on, we settle the following notation:

$$\delta_1 = \frac{C_1}{E_1} > 1, \quad \delta_2 = \frac{C_2}{E_2} > 1, \quad \delta = \delta_1 \delta_2 > 1 \tag{2.2}$$

and

$$K_\omega = \frac{E_2 \omega_1 + C_1 \omega_2}{E_1 E_2} > 0. \tag{2.3}$$

The constant K_ω will be called the *twisting number* of Γ . From now on, denote by $\mathfrak{X}_{\text{Byk}}^r(\mathbb{S}^3)$ the set of two-parameter families of C^r -vector fields that satisfy the conditions **(P1)**–**(P8)**. The parameters A and λ are supposed to be small.

2.4. The results. According to [31], we may draw, in the first quadrant, two smooth curves, the graphs of h_1 and h_2 , such that:

- (1) $h_1(K_\omega) = \frac{1}{\sqrt{1 + K_\omega^2}}$ and $h_2(K_\omega) = \frac{\exp\left(\frac{6\pi}{K_\omega}\right) - 1}{\exp\left(\frac{6\pi}{K_\omega}\right) - 1/6}$;
- (2) the region below the graph of h_1 corresponds to flows having an invariant and attracting torus with *zero topological entropy* (regular dynamics);
- (3) the region above the graph of h_2 corresponds to vector fields whose flows exhibit *rotational horseshoes* in the sense of Passegi *et al* [26] – see (A.5).

Under some conditions on the parameters and on the eigenvalues of the linearisation of the vector field at the saddle-foci, the author of [31] proved the existence of Hénon-like strange attractors near the “ghost” of the Bykov attractor:

Theorem 2.1 ([31], adapted). *Let $f_{(A,\lambda)} \in \mathfrak{X}_{\text{Byk}}^3(\mathbb{S}^3)$. Fix $K_\omega^0 > 0$. In the bifurcation diagram $(A, \frac{\lambda}{A})$, where (A, λ) is such that $h_1(K_\omega^0) < \frac{\lambda}{A} < h_2(K_\omega^0)$, there exists a positive measure set Δ of parameter values, so that for every $\lambda/A \in \Delta$, the flow of (2.1) admits a strange attractor of Hénon-type with an ergodic SRB measure (see (A.6)).*

In this paper, we illustrate the typical bifurcations from an attracting torus to strange attractors, with a particular example (see Section 3).

3. THE EXAMPLE

We construct an explicit two parametric family of vector fields $f_{(\tau_1, \tau_2)}$ in $\mathbb{S}^3 \subset \mathbb{R}^4$ whose organizing center satisfies **(P1)**–**(P5)**. Our construction is based on properties of *differential equations with symmetry* (see (A.7)); we also refer the reader to [13, 15, 16] for more information on the subject.

3.1. The system. For $\tau_1, \tau_2 \in [0, 1]$, our object of study is the two-parameter family of vector fields on \mathbb{R}^4

$$x = (x_1, x_2, x_3, x_4) \in \mathbb{R}^4 \quad \mapsto \quad f_{(\tau_1, \tau_2)}(x)$$

defined for each $x = (x_1, x_2, x_3, x_4) \in \mathbb{R}^4$ by

$$\begin{cases} \dot{x}_1 = x_1(1 - r^2) - \omega x_2 - \alpha x_1 x_4 + \beta x_1 x_4^2 + \tau_2 x_1 x_3 x_4 \\ \dot{x}_2 = x_2(1 - r^2) + \omega x_1 - \alpha x_2 x_4 + \beta x_2 x_4^2 \\ \dot{x}_3 = x_3(1 - r^2) + \alpha x_3 x_4 + \beta x_3 x_4^2 + \tau_1 x_4^3 - \tau_2 x_1^2 x_4 \\ \dot{x}_4 = x_4(1 - r^2) - \alpha(x_3^2 - x_1^2 - x_2^2) - \beta x_4(x_1^2 + x_2^2 + x_3^2) - \tau_1 x_3 x_4^2 \end{cases} \quad (3.1)$$

where

$$\dot{x}_i = \frac{\partial x_i}{\partial t}, \quad r^2 = x_1^2 + x_2^2 + x_3^2 + x_4^2$$

and

$$\omega > 0, \quad \beta < 0 < \alpha, \quad \beta^2 < 8\alpha^2 \quad \text{and} \quad |\beta| < |\alpha|.$$

Remark 3.1. The nature of the perturbations, which depend on τ_1 and τ_2 , has been listed in Appendix B of [29].

The unit sphere $\mathbb{S}^3 \subset \mathbb{R}^4$ is invariant under the corresponding flow and every trajectory with nonzero initial condition is forward asymptotic to it (cf. [29]). Indeed, if $\langle \cdot, \cdot \rangle$ denotes the usual inner product in \mathbb{R}^4 , then it is easy to check that:

Lemma 3.2. *For every $x \in \mathbb{S}^3$ and $\tau_1, \tau_2 \in [0, 1]$, we have $\langle f_{(\tau_1, \tau_2)}(x), x \rangle = 0$.*

We are interested in dynamics on a compact boundaryless manifold, in order to have control of the long-time existence and behaviour of solutions. Moreover, the origin is repelling since all eigenvalues of $Df_{(\tau_1, \tau_2)}$ at the origin have positive real part.

3.2. The organizing center ($\tau_1 = \tau_2 = 0$). The vector field $f_{(0,0)}$ is equivariant under the action of the compact Lie group $\mathbb{SO}(2)(\gamma_\psi) \oplus \mathbb{Z}_2(\gamma_2)$, where $\mathbb{SO}(2)(\gamma_\psi)$ and $\mathbb{Z}_2(\gamma_2)$ act on \mathbb{R}^4 as

$$\gamma_\psi(x_1, x_2, x_3, x_4) = (x_1 \cos \psi - x_2 \sin \psi, x_1 \sin \psi + x_2 \cos \psi, x_3, x_4), \quad \psi \in [0, 2\pi]$$

given by a phase shift $\theta \mapsto \theta + \psi$ in the first two coordinates, and

$$\gamma_2(x_1, x_2, x_3, x_4) = (x_1, x_2, -x_3, x_4).$$

By construction, τ_1 is the controlling parameter of the $\mathbb{Z}_2(\gamma_2)$ -symmetry breaking and τ_2 controls the $\mathbb{SO}(2)(\gamma_\psi)$ -symmetry breaking but keeping the $\mathbb{SO}(2)(\gamma_\pi)$ -symmetry², where $\gamma_\pi(x_1, x_2, x_3, x_4) = (-x_1, -x_2, x_3, x_4)$. See the following table for the symmetries preserved according to parameters:

| Parameters | Symmetries preserved |
|--------------------------------------|---|
| $\tau_1 = \tau_2 = 0$ | $\mathbb{SO}(2)(\gamma_\psi) \oplus \mathbb{Z}_2(\gamma_2)$ |
| $\tau_1 > 0$ and $\tau_2 = 0$ | $\mathbb{SO}(2)(\gamma_\psi)$ |
| $\tau_1 = 0$ and $\tau_2 > 0$ | $\mathbb{Z}_2(\gamma_\pi) \oplus \mathbb{Z}_2(\gamma_2)$ |
| $\tau_1 > 0$ and $\tau_1 \gg \tau_2$ | $\mathbb{Z}_2(\gamma_\pi)$ |

Table 1: Types of symmetry-breaking according to the parameters.

²Observe that $\mathbb{SO}(2)(\gamma_\pi) \cong \mathbb{Z}_2(\gamma_\pi)$, *i.e.* the action of both Lie groups on \mathbb{R}^4 are isomorphic.

When restricted to the sphere \mathbb{S}^3 , for every $\tau_1, \tau_2 \in [0, 1]$, the flow of $f_{(\tau_1, \tau_2)}$ has two equilibria

$$O_1 = (0, 0, 0, +1) \quad \text{and} \quad O_2 = (0, 0, 0, -1),$$

which are hyperbolic saddle-foci with different *Morse indices* (dimension of the unstable manifold). The linearization of $f_{(0,0)}$ at O_1 and O_2 has eigenvalues

$$-(\alpha - \beta) \pm \omega i, \alpha + \beta \quad \text{and} \quad (\alpha + \beta) \pm \omega i, -(\alpha - \beta)$$

respectively. As depicted in Figure 1, when restricted to \mathbb{S}^3 , in these coordinates, the 1D-connections are given by:

$$W^u(O_1) \cap \mathbb{S}^3 = W^s(O_2) \cap \mathbb{S}^3 = \text{Fix}(\mathbb{S}\mathbb{O}(2)(\gamma_\psi)) \cap \mathbb{S}^3 = \{(x_1, x_2, x_3, x_4) : x_1 = x_2 = 0, x_3^2 + x_4^2 = 1\}$$

and the 2D-connection is contained in

$$W^u(O_2) \cap \mathbb{S}^3 = W^s(O_1) \cap \mathbb{S}^3 = \text{Fix}(\mathbb{Z}_2(\gamma_2)) \cap \mathbb{S}^3 = \{(x_1, x_2, x_3, x_4) : x_1^2 + x_2^2 + x_4^2 = 1, x_3 = 0\}.$$

The two-dimensional invariant manifolds are contained in the two-sphere $\text{Fix}(\mathbb{Z}_2(\gamma_2)) \cap \mathbb{S}^3$. It is precisely this symmetry that forces the two-invariant manifolds $W^u(O_2)$ and $W^s(O_1)$ to coincide. In what follows, we denote by Γ the *heteroclinic network* formed by the two equilibria, the two connections $[O_1 \rightarrow O_2]$ and the sphere $[O_2 \rightarrow O_1]$ (see Figure 1). The network may be decomposed into two cycles.

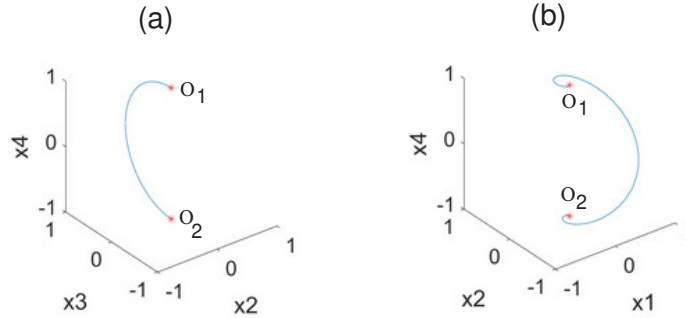


FIGURE 1. Organizing center. (a) One 1D-connection from O_1 to O_2 . (b) One trajectory within the 2D-connection from O_2 to O_1 . Flow of (3.1) with $\tau_1 = \tau_2 = 0$, $\omega = 1$, $\alpha = 1$ and $\beta = -0.1$, $t \in [0, 10000]$. (a) Initial condition $(0; 0; 0.01; 0.99)$ near $W^s(O_1)$; projection into the coordinates (x_2, x_3, x_4) . (b) Initial condition $(0.1; 0.1; 0; -0.99)$ near $W^u(O_2)$; projection into the coordinates (x_1, x_2, x_4) .

Proposition 1 of [29] shows that, keeping $\tau_1 = \tau_2 = 0$, the equilibria O_1 and O_2 have the same *chirality* (details in (A.3)). Therefore:

Lemma 3.3. *If $\tau_1 = \tau_2 = 0$, the flow of (3.1) satisfies (P1)–(P5) described in Section 2.*

In summary, when $\tau_1 = \tau_2 = 0$, the flow of (3.1) exhibits an asymptotically stable heteroclinic network Γ associated to O_1 and O_2 , numerically shown in Figure 2. Throughout the construction and discussion, the parameters τ_1 and τ_2 play the role of A and λ , respectively, of (P6)–(P7), after possible rescaling.

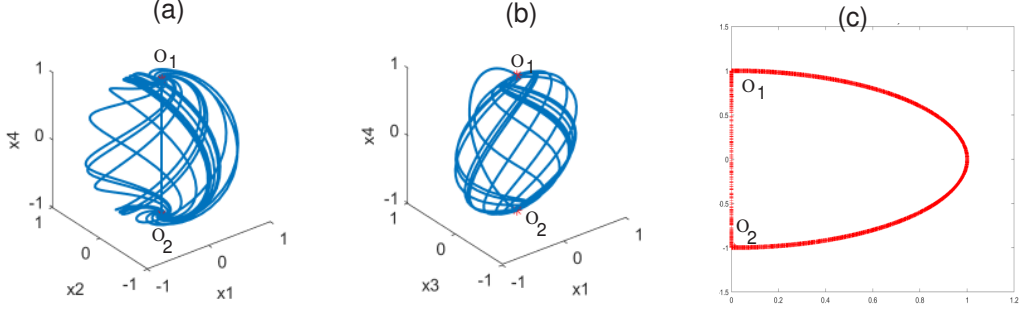


FIGURE 2. Flow of (3.1) of the trajectory with initial condition $(0.1; 0.1; 0; -0.99)$ near $W^u(O_2)$, with $\tau_1 = \tau_2 = 0$, $\omega = 1$, $\alpha = 1$ and $\beta = -0.1$, $t \in [0, 10000]$. (a) Projection into the coordinates (x_1, x_2, x_4) . (b) Projection into the coordinates (x_1, x_3, x_4) . (c) Projection into the section $x_1 = x_2 = 0$.

3.3. Notation. As in Subsection 2.3, we set the following notation:

$$C_1 = C_2 = \alpha - \beta > 0, \quad E_1 = E_2 = \alpha + \beta > 0, \quad \delta_1 = \delta_2 = \frac{\alpha - \beta}{\alpha + \beta} > 1 \quad (3.2)$$

and

$$K = \frac{2\alpha}{(\alpha + \beta)^2} > 0 \quad \text{and} \quad K_\omega = \frac{2\alpha\omega}{(\alpha + \beta)^2} > 0. \quad (3.3)$$

3.4. $\mathbb{Z}_2(\gamma_2)$ -symmetry breaking ($\tau_1 > \tau_2 = 0$). In this scenario, the heteroclinic network Γ is broken because the symmetry $\mathbb{Z}_2(\gamma_2)$ is broken. The flow of $f_{(\tau_1, 0)}$ leaves the unit sphere \mathbb{S}^3 invariant and globally attracting since the perturbations are tangent to \mathbb{S}^3 [29, Appendix B]. We are going to present analytical evidences that an attracting two-torus is born.

Since the system $\dot{x} = f_{(\tau_1, 0)}(x)$ is still $\mathbb{SO}(2)(\gamma_\psi)$ -equivariant (see Table 1), we may define the quotient flow on $\mathbb{S}^3/\mathbb{SO}(2)(\gamma_\psi)$ (see [32]) and we get the following differential equation:

$$\begin{cases} \dot{\rho} = \rho(1 - R^2) - \alpha\rho x_4 + \beta\rho x_4^2 \\ \dot{x}_3 = x_3(1 - R^2) + \alpha x_3 x_4 + \beta x_3 x_4^2 + \tau_1 x_4^3 \\ \dot{x}_4 = x_4(1 - R^2) - \alpha(x_3^2 - \rho^2) - \beta x_4(\rho^2 + x_3^2) - \tau_1 x_3 x_4^2 \end{cases} \quad (3.4)$$

where

$$R^2 = \rho^2 + x_3^2 + x_4^2 \quad \text{and} \quad \rho^2 = x_1^2 + x_2^2.$$

The equations (3.4), restricted to the unit two-sphere \mathbb{S}^2 (*i.e.* $R^2 = 1$), simplify to

$$\begin{cases} \dot{\rho} = \alpha\rho x_4 + \beta\rho x_4^2 \\ \dot{x}_3 = \alpha x_3 x_4 + \beta x_3 x_4^2 + \tau_1 x_4^3 \\ \dot{x}_4 = -\alpha(x_3^2 - \rho^2) - \beta x_4(\rho^2 + x_3^2) - \tau_1 x_3 x_4^2, \end{cases} \quad (3.5)$$

a differential equation that may be *reduced* to the following planar system:

$$\begin{cases} \dot{x}_3 = \alpha x_3 x_4 + \beta x_3 x_4^2 + \tau_1 x_4^3 \\ \dot{x}_4 = \alpha(1 - 2x_3^2 - x_4^2) + \beta x_4(x_4^2 - 1) - \tau_1 x_3 x_4^2. \end{cases} \quad (3.6)$$

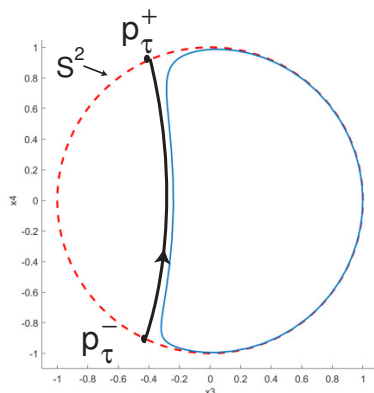


FIGURE 3. Flow of (3.6) of the trajectory with initial condition $(x_3, x_4) = (0; -0.99)$ near $W^u(p_\tau^-)$, with $\alpha = 1$, $\beta = -0.1$ and $\tau_1 = 0.5$, $t \in [0, 10000]$. The blue closed curve of (3.6) is stable. The red dashed line represents the unit circle.

For $\tau_1 = 0$, the points $p_0^\pm = (0, \pm 1) \in \mathbb{S}^1$ are hyperbolic equilibria for (3.6). For $\tau_1 \neq 0$, let p_τ^\pm be their *hyperbolic continuation*. Using the Poincaré-Bendixson Theorem, Aguiar [5] proved that:

Lemma 3.4 ([5], adapted). *For $\tau_1 > 0$, the flow of system (3.6) has one stable periodic solution, which emerges from the breaking of the attracting network associated to the equilibria p_0^\pm . The unstable manifold of p_τ^- does not intersect the stable manifold of p_τ^+ .*

The stable periodic solution of Lemma 3.4 is illustrated in Figure 3. By the $\mathbb{SO}(2)(\gamma_\psi)$ -equivariance, this sink lifts to an attracting torus (details of the *lifting process* is given in (A.7)). Therefore:

Corollary 3.5. *For $\tau_1 > 0$ and $\tau_2 = 0$, close to the “ghost” of the attracting network Γ , the flow of (3.1) has an attracting invariant two-torus, which is normally hyperbolic.*

From the theory for normally hyperbolic manifolds developed in [18], the torus persists under small smooth perturbations. The numerical evidence of Figure 4(a) suggests that the dynamics restricted to the torus is *quasi-periodic*.

3.5. $\mathbb{Z}_2(\gamma_2)$ and $\mathbb{SO}(2)(\gamma_\psi)$ -symmetry breaking ($\tau_1 \gg \tau_2 > 0$). We now explore the case $\tau_1 \gg \tau_2 > 0$. Once again, the flow of $f_{(\tau_1, \tau_2)}$ leaves the unit sphere \mathbb{S}^3 invariant and globally attracting since the perturbations are tangent to \mathbb{S}^3 – [29, Appendix B]. Although we break the $\mathbb{SO}(2)(\gamma_\psi)$ -equivariance, the $\mathbb{SO}(2)(\gamma_\pi)$ -symmetry is preserved. This is why the connections lying in $x_1 = x_2 = 0$ persist (\Rightarrow **(P6)** holds). Using now Lemma 3.4, by construction, we have:

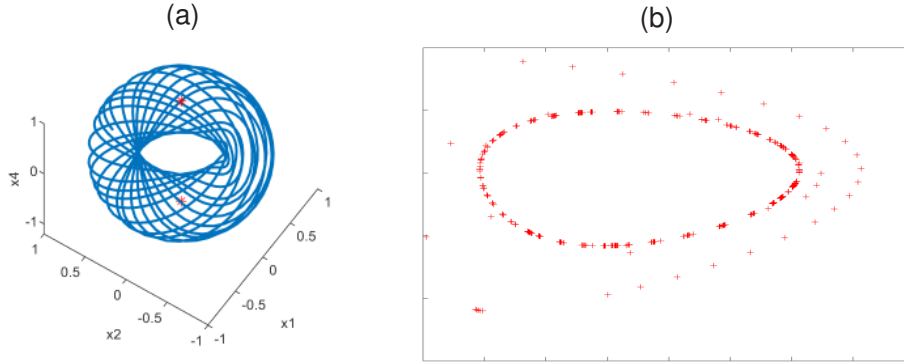


FIGURE 4. Projection of the flow of (3.1) of the trajectory with initial condition $(0.1; 0.1; 0; -0.99)$ near $W^u(O_2)$, with $\tau_1 = 0.5$, $\tau_2 = 0$, $\omega = 1$, $\alpha = 1$ and $\beta = -0.1$, $t \in [0, 10000]$. (a) Projection into the coordinates (x_1, x_2, x_4) . (b) Projection into the section $x_1 = x_2 = 0$.

Lemma 3.6. *For $\tau_1 \geq 0$ and $\tau_2 > 0$ small enough such that $\tau_1 \gg \tau_2 > 0$, the flow of (3.1) satisfies (P6)–(P7).*

Numerical simulations of (3.1) for $\tau_1 \gg \tau_2 > 0$ suggest the existence of regular and chaotic behaviour in the region of transition from regular dynamics (attracting torus) to rotational saturated horseshoes (see (A.4) and (A.5)). Chaotic attractors with one positive Lyapunov exponent seem to exist, as suggested by the yellow regions of Figure 5. Using the Matlab software (R2019b, MathWorks, Natick, MA, USA), we have been able to compute the bifurcation diagram presented in Figure 5, whose analysis is the goal of next section.

4. TORUS-BREAKDOWN AND STRANGE ATTRACTORS: THEORY AND NUMERICS

The destruction of the torus of Corollary 3.5 takes place according to the scenario described in [1, 3, 4, 10]. In this section, we describe the (generic) mechanism to break an attracting two-dimensional torus and we relate this theory with our numerics, which agree quite well. Before going further, we introduce some terminology.

Let \mathcal{T} be a neighborhood of the Bykov attractor Γ which exists for (3.1) when $\tau_1 = \tau_2 = 0$. Let Σ be a cross section to Γ . There is $\varepsilon > 0$ (small) such that the first return map $\mathcal{F}_{(\tau_1, \tau_2)}$ to a subset of Σ is well defined, for $\tau_1, \tau_2 < \varepsilon$ (cf. [31]). We assume that the intersection of the torus with the cross section Σ is a curve diffeomorphic to a circle, as depicted in Figure 4(b).

The choice of parameters in Section 3 lets us build the bifurcation diagram in the plane of the parameters (τ_1, τ_2) in the domain

$$\{0 \leq \tau_1 < \varepsilon, \quad 0 < \tau_2 < \tau_2^0\},$$

for $0 < \tau_2^0 \ll \varepsilon$. Within this region, it is possible to define an *Arnold tongue* [10], denoted by \mathcal{T}_k , adjoining the horizontal axis at a point A_k where k is an integer. Inside this *tongue* (*resonant wedge*), for small τ_2 , there coexist at least a pair of fixed points for the Poincaré map $\mathcal{F}_{(\tau_1, \tau_2)}$, whose corresponding trajectories share the same *rotation number* [1, 17]. As illustrated in Figure 5 (upper part), we suppose the existence of two pairs of fixed points: Q_k^1 , Q_k^2 (saddles) and P_k^1 , P_k^2 (sinks).

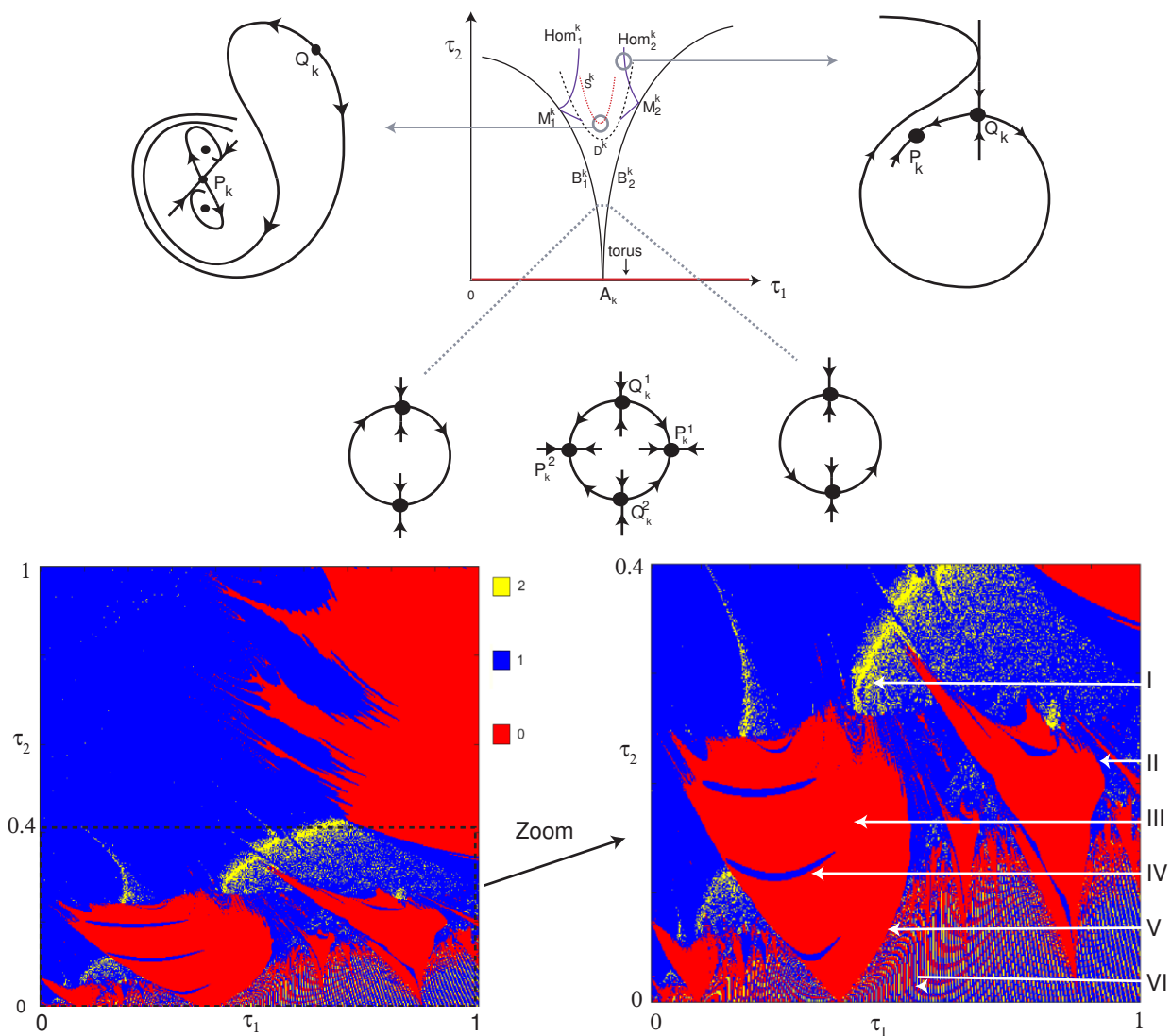


FIGURE 5. Bifurcation diagram for equation (3.1) with $\alpha = 1$, $\beta = -0.1$ and $\omega = 1$, corresponding to the trajectory with initial condition $(0.1; 0.1; 0; -0.99)$ near $W^u(O_2)$, $t \in [0, 3750]$. Upper part: theoretical scheme [10]. Lower part: (real) bifurcation diagram. Each point is colored according to the number of non-negative Lyapunov exponents of the orbit: yellow (2), blue (1) and red (0), corresponding to an ω -limit including a strange attractor or an attracting two-torus, a limit cycle or a fixed point, respectively.

The borders of \mathcal{T}_k are bifurcation curves B_1^k and B_2^k on which each pair of fixed points merge into a *saddle-node*. These curves might touch the corresponding curves of other tongue, meaning that there are parameter values for which periodic solutions with different rotation number might coexist. The points M_1^k and M_2^k correspond to *homoclinic cycles to a saddle-node*: below these points, in B_1^k and B_2^k , the limit set of $W^u(Q_k^1)$ is the saddle-node itself.

Above the points M_1^k and M_2^k , the maximal invariant set is not homeomorphic to a circle. In the bifurcation diagram, there is also a curve, say D^k , above which the invariant torus no longer exists due to a *period doubling bifurcation* [9]. After the period doubling has occurred, the torus is destroyed.

Continuing the process of dissecting an Arnold tongue, the authors of [1, 9] describe generic mechanisms by which the invariant and attracting torus is destroyed. Two of them are revived in the next result and involve homoclinic tangencies – routes [PA] and [PB] of [9].

Theorem 4.1 ([1, 9], adapted). *For $K_\omega^0 > 0$ fixed, in the bifurcation diagram (τ_1, τ_2) , within \mathcal{T}_k ,*

- (1) *there are two curves Hom_1^k and Hom_2^k corresponding to a homoclinic tangency associated to a dissipative periodic point of the first return map $\mathcal{F}_{(\tau_1, \tau_2)}$.*
- (2) *there is one curve S^k corresponding to a homoclinic tangency (of third class) associated to a dissipative periodic point of the first return map $\mathcal{F}_{(\tau_1, \tau_2)}$.*

The lines S^k , Hom_1^k , Hom_2^k are shown in Figure 5.

Fix $i \in \{1, 2\}$ and assume that $Q_k^i \equiv Q_k$. Along the bifurcation curves Hom_1^k and Hom_2^k , one observes a homoclinic contact of the components $W^s(Q_k)$ and $W^u(Q_k)$, where Q_k is a dissipative saddle³. The curves Hom_1^k and Hom_2^k divide the region above D^k into two regions with simple and complex dynamics. In the zone above the curves Hom_1^k and Hom_2^k , there is a fixed point Q_k exhibiting a transverse homoclinic intersection, and thus the corresponding map $\mathcal{F}_{(\tau_1, \tau_2)}$ exhibits nontrivial hyperbolic chaotic sets (horseshoes). Other stable points of large period exist in the region above the curves Hom_1^k and Hom_2^k since the homoclinic tangencies arising in these lines are generic – *Newhouse phenomena* [12, 25]. Using now [24], there exists a positive measure set Δ of parameter values, so that for every $\tau_1/\tau_2 \in \Delta$, the map $\mathcal{F}_{(\tau_1, \tau_2)}$ admits a strange attractor of Hénon-type with an ergodic SRB measure (cf. (A.6)). This is observable in the two yellow regions leaving the *Arnold tongues* of Figure 5 (lower part). The formation of the Hénon-like strange attractor is suggested in Figure 6.

The curve S^k of Theorem 4.1 corresponds to a homoclinic tangency of third class, meaning that there are tangencies associated to the fixed points emerged from the period-doubling bifurcation at D^k . This line corresponds to the boundary between the red and blue lines in Figure 5 (lower image), within the resonant wedge. We conjecture that this line is a consequence of an exponentially small wedge associated to a *Bogdanov-Takens* bifurcation [34, Fig. 3]. After crossing the curve D_k (from below), the invariant curve no longer exists. Of course, the individual solutions (orbits) remain smooth.

Yellow narrow regions of Figure 5, near the horizontal axis, are due to the existence of a set of parameters for which the torus-flow is *irrational*; the corresponding orbit is unlocked and winds without bound around the torus. In Figure 5, we also observe *frequency locking regions* (red regions), regions dominated by a sink (blue) as well as regions with positive entropy (yellow). The number of connected components with which the strange attractors intersect the cross-section is not specified nor is the size of their basins of attraction.

For $\tau_1, \tau_2 > 0$, the flow associated to $f_{(\tau_1, \tau_2)}$ leaves \mathbb{S}^3 invariant and globally attracting, which explains the regularity of borders of the different images in Figure 6. In Figure 7, we

³One saddle O is dissipative if $0 < |\det D\mathcal{F}_{(\tau_1, \tau_2)}(O)| < 1$ (i.e. $\mathcal{F}_{(\tau_1, \tau_2)}$ is contracting for any small neighbourhood of O). Note that, for small $\tau_1, \tau_2 > 0$, the first return map $\mathcal{F}_{(\tau_1, \tau_2)}$ is contracting.

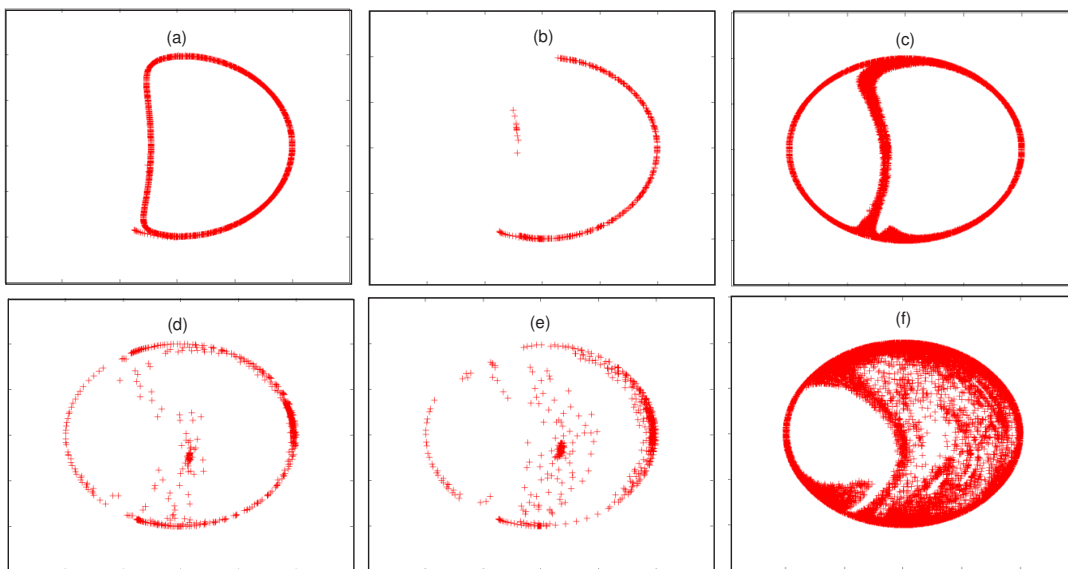


FIGURE 6. Projection of the flow of (3.1) of the trajectory with initial condition $(0.1; 0.1; 0; -0.99)$ with $\alpha = 1$, $\beta = -0.1$, $\tau_1 = 0.3$, $\omega = 1$ and $\tau_2 = 0$ (a); $\tau_2 = 0.1$ (b), $\tau_2 = 0.2$ (c), $\tau_2 = 0.3$ (d), $\tau_2 = 0.4$ (e), and $\tau_2 = 0.5$ (f).

give an additional generic image of the typical picture of *Hénon-like attractor* which appears near the Bykov attractor when all symmetries are broken, as well as the sphere-invariance. The plot has been performed for the vector field $f_{(0,0)}$ of (3.1) with the following perturbing term:

$$(x_1 x_3 x_4, -x_1 x_2^2, x_3^3, -x_1 x_3 x_4). \quad (4.1)$$

The resulting vector field breaks all symmetries, all well as the sphere invariance. The unstable manifold of the saddle Q_k has crossed the non-leading stable manifold of the periodic orbit.

Possible interpretation of Figure 5.

- I** → Homoclinic bifurcations; Hénon-like strange attractors.
- II** → Sink.
- III** → Resonant wedge (Arnold tongue).
- IV** → Hopf bifurcation.
- V** → Saddle-node bifurcation (border of the Arnold tongue).
- VI** → Irrational torus (thin yellow region).

Technicalities of the numerics. Since $W^u(O_2)$ plays an essential role in the construction of the Hénon-like strange attractor [31], we chose $(0.1; 0.1; 0; -0.99) \in \mathbb{R}^4$ to grasp the main dynamical properties of the maximal attracting set of (3.1). Although the system (3.1) lives in \mathbb{R}^4 , the analysis may be performed in the sphere \mathbb{S}^3 since it is globally attracting. According to [33, pp. 287], for a three-dimensional continuous dissipative flow, the only possible spectra

and the attractors they describe depend of the sign of their Lyapunov exponents:

- $(-, -, -)$ → the ω -limit of the corresponding orbit contains a fixed point;
- $(0, -, -)$ → the ω -limit of the corresponding orbit is a limit cycle;
- $(+, 0, -)$ → the ω -limit of the corresponding orbit is a chaotic attractor;
- $(0, 0, -)$ → the ω -limit of the corresponding orbit is an attracting 2-torus.

The parameter plane (τ_1, τ_2) of Figure 5 is scanned with a sufficiently small step along each coordinate axes. The software evaluates at each parameter value how many Lyapunov exponents along the orbit with initial condition $(0.1; 0.1; 0; -0.99)$ are non-negative. Then, the parameter is painted according to the following rules: red for 0, blue for 1, yellow for 2. To estimate the complete Lyapunov spectra, we use the algorithm for differential equations introduced in [33] with a Taylor series integrator.

Remark 4.2. Observe that yellow regions of Figure 5 mean that the ω -limit of the corresponding orbit may be either a strange attractor (I) or an attracting two-torus (VI). The first seems to be prevalent; the second is not.

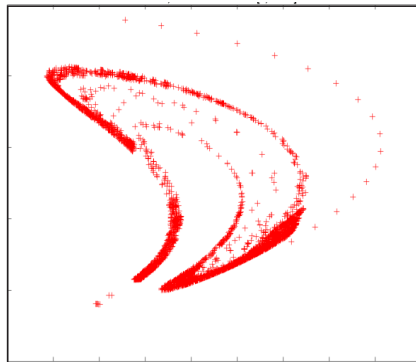


FIGURE 7. Breaking the invariant curve of Figure 4(b) on the section $x_1 = x_2 = 0$. Projection of the flow of (4.1) of the trajectory with initial condition $(0.1; 0.1; 0; -0.99)$ and $t \in [0, 10000]$. The perturbation breaks all the symmetries, as well as the sphere invariance.

5. DISCUSSION AND FINAL REMARKS

The goal of this paper is to construct explicitly a two-parameter family of polynomial differential equations $\dot{x} = f_{(\tau_1, \tau_2)}(x)$ in the three-dimensional sphere \mathbb{S}^3 , in which each parameter controls a type of symmetry-breaking. Depending on the parameters, different dynamical regimes have been identified both analytically and numerically. We have stressed the emergence of strange attractors from an attracting heteroclinic network, a *route to chaos* which has been a recurrent concern on nonlinear dynamics during the last decades. Along this discussion we compare our results to what is known for other models in the literature.

The flow of $\dot{x} = f_{(0,0)}(x)$ has an attracting heteroclinic network Γ with a non-empty basin of attraction \mathcal{U} . We have studied the global transition of the dynamics from $\dot{x} = f_{(0,0)}(x)$ to a smooth two-parameter family $\dot{x} = f_{(\tau_1, \tau_2)}(x)$ that breaks part of the network. For small

perturbations, the set \mathcal{U} is still positively invariant. When $\tau_1, \tau_2 \neq 0$, the one-dimensional connections persist due to the remaining symmetry and, as a consequence of Kupka-Smale Theorem, the two-dimensional invariant manifolds are generically transverse (either intersecting or not).

When $\tau_2 > \tau_1 \geq 0$, the two-dimensional invariant manifolds intersect transversely, giving rise to a complex network, that consists of a union of Bykov cycles [11], contained in \mathcal{U} . The dynamics in the maximal invariant set contained in \mathcal{U} , contains, but does not coincide with, the suspension of horseshoes accumulating on the heteroclinic network described in [6, 20, 22, 27, 28, 29]. In addition, close to the organizing center ($\tau_1 = \tau_2 = 0$), it contains infinitely many heteroclinic tangencies and attracting limit cycles with long periods, coexisting with sets with positive entropy, giving rise to the so called *quasi-stochastic attractors*. The sinks in a quasi-stochastic attractor have long periods and narrow basins of attraction, and they are hard to be observed in applied problems [2, 14].

The scenario $\tau_1 > \tau_2 \geq 0$ corresponds to the case where the two-dimensional invariant manifolds do not intersect. Although the network associated to the equilibria is destroyed, complex dynamics appears near its “ghost”. In the present article, it is shown that the perturbed system may manifest regular behaviour corresponding to the existence of a smooth invariant torus, and may also have chaotic regimes. In the region of transition from regular behaviour to chaotic dynamics, using known results about *Arnold tongues*, we illustrate the existence of lines with homoclinic tangencies to dissipative periodic solutions, responsible for the existence of persistent strange attractors nearby (cf. region (I) of Figure 5). Numerics agree quite well with the theory described in [31]. Persistence of chaotic dynamics is physically relevant because it means that the phenomenon is numerically observable with positive probability.

In the fully asymmetric case, the general study of (3.1) seems to be analytically untreatable. We have been able to predict qualitative features of the dynamics of the perturbed vector field by assuming that the perturbation is very close to the organizing center. Symmetry plays two roles: first, it creates flow-invariant subspaces where non-transverse heteroclinic connections are persistent, and hence cycles are robust in this context; second, we use the proximity of the fully symmetric case to capture global dynamics. Symmetry constrains the geometry of the invariant manifolds of the saddle-foci and allows us some control of their relative positions. This is an important advantage of studying systems close to symmetry.

In a subsequent paper we will treat some other aspects of this class of examples, in particular partial mode-locking, frequently associated with the existence of homotopically non-trivial invariant circles on the torus. We conjecture that the boundaries of partial mode-locked regions involve *Bodganov-Takens bifurcations* in the parameter space $(\tau_1, \tau_2, K_\omega)$.

ACKNOWLEDGEMENTS

AR was partially supported by CMUP (UID/MAT/00144/2019), which is funded by FCT with national (MCTES) and European structural funds through the programs FEDER, under the partnership agreement PT2020. AR also acknowledges financial support from Program INVESTIGADOR FCT (IF/00107/2015).

REFERENCES

- [1] V.S. Afraimovich, L.P. Shilnikov. *On invariant two-dimensional tori, their breakdown and stochasticity* in: Methods of the Qualitative Theory of Differential Equations, Gor’kov. Gos. University (1983), 3–26. Translated in: Amer. Math. Soc. Transl., (2), vol. 149 (1991), 201–212.

- [2] V.S. Afraimovich, L.P. Shilnikov. *Strange attractors and quasiattractors*, Nonlinear Dynamics and Turbulence. G.I. Barenblatt, G. Iooss, D.D. Joseph (Eds.), Pitman, Boston (1983) 1–51.
- [3] V.S. Afraimovich, S-B Hsu, H. E. Lin. *Chaotic behavior of three competing species of May-Leonard model under small periodic perturbations*, Int. J. Bif. Chaos, 11(2) (2001) 435–447
- [4] V. S. Afraimovich, S. B. Hsu. *Lectures on Chaotic Dynamical Systems*, American Mathematical Society and International Press, 2002.
- [5] M. Aguiar. *Vector fields with heteroclinic networks*, Ph.D. thesis, Departamento de Matemática Aplicada, Faculdade de Ciências da Universidade do Porto, 2003.
- [6] M.A.D. Aguiar, S.B.S.D. Castro, I.S. Labouriau. *Dynamics near a heteroclinic network*, Nonlinearity 18 (2005) 391–414.
- [7] M.A.D. Aguiar, S.B.S.D. Castro, I.S. Labouriau. *Simple vector fields with complex behaviour*, International Journal of Bifurcation and Chaos 16(2), (2006), 369–381.
- [8] M.A.D. Aguiar, I.S. Labouriau, A.A.P. Rodrigues. *Switching near a heteroclinic network of rotating nodes*, Dyn. Sys. Int. J. 25(1) (2010) 75–95.
- [9] V. Anishchenko, M. Safonova, L Chua. *Confirmation of the Afraimovich-Shilnikov torus-breakdown theorem via a torus circuit*, IEEE Transactions on Circuits and Systems I: Fundamental Theory and Applications, 40(11), (1993) 792–800.
- [10] D. Aronson, M. Chory, G. Hall, R. McGehee. *Bifurcations from an invariant circle for two-parameter families of maps of the plane: a computer-assisted study*, Communications in Mathematical Physics, 83(3), (1982) 303–354.
- [11] V.V. Bykov. *Orbit Structure in a neighborhood of a separatrix cycle containing two saddle-foci*, Amer. Math. Soc. Transl. 200 (2000) 87–97.
- [12] E. Colli. *Infinitely many coexisting strange attractors*, Ann. Inst. H. Poincaré, 15 (1998) 539–579.
- [13] M. Golubitsky, I. Stewart. *The Symmetry Perspective*, Birkhauser, 2000
- [14] S.V. Gonchenko, L.P. Shilnikov, D.V. Turaev. *Quasiattractors and homoclinic tangencies*, Computers Math. Applic. 34(2–4) (1997) 195–227.
- [15] J. Guckenheimer, P. Holmes. *Nonlinear Oscillations, Dynamical Systems, and Bifurcations of Vector Fields*, Applied Mathematical Sciences 42, Springer-Verlag, 1983.
- [16] J. Guckenheimer, P. Worfolk. *Instant chaos*, Nonlinearity 5 (1991) 1211–1222.
- [17] M. Herman. *Mesure de Lebesgue et Nombre de Rotation*, Lecture Notes in Math., vol. 597, Springer, 1977, 271–293.
- [18] M. W. Hirsch C. Pugh, M. Shub. *Invariant manifolds*, Bull. Amer. Math. Soc. 76 (1970), no. 5, 1015–1019.
- [19] A.J. Homburg, B. Sandstede. *Homoclinic and Heteroclinic Bifurcations in Vector Fields*, Handbook of Dynamical Systems 3, North Holland, Amsterdam, 379–524, 2010.
- [20] J. Knobloch, J.S.W. Lamb, K.N. Webster. *Using Lin’s method to solve Bykov’s problems*, J. Diff. Eqs. 257(8) (2014) 2984–3047.
- [21] W.S. Koon, M. Lo, J. Marsden, S. Ross. *Heteroclinic connections between periodic orbits and resonance transition in celestial mechanics*, Control and Dynamical Systems Seminar, California Institute of Technology, Pasadena, California, 1999.
- [22] I.S. Labouriau, A.A.P. Rodrigues. *Global generic dynamics close to symmetry*, J. Diff. Eqs. 253(8) (2012) 2527–2557.
- [23] I.S. Labouriau, A.A.P. Rodrigues. *Dense heteroclinic tangencies near a Bykov cycle*, J. Diff. Eqs. 259(12) (2015) 5875–5902.
- [24] L. Mora, M. Viana. *Abundance of strange attractors*, Acta Math. 171(1) (1993) 1–71.
- [25] S.E. Newhouse. *The abundance of wild hyperbolic sets and non-smooth stable sets for diffeomorphisms*, Publ. Math. Inst. Hautes Études Sci. 50 (1979) 101–151.
- [26] A. Passeggi, R. Potrie, M. Sambarino. *Rotation intervals and entropy on attracting annular continua*, Geometry & Topology 22(4), 2145–2186, 2018.
- [27] A.A.P. Rodrigues. *Persistent switching near a heteroclinic model for the geodynamo problem*, Chaos, Solitons & Fractals 47 (2013) 73–86.
- [28] A.A.P. Rodrigues. *Repelling dynamics near a Bykov cycle*, J. Dyn. Diff. Eqs. 25(3) (2013) 605–625.
- [29] A.A.P. Rodrigues, I.S. Labouriau. *Spiralling dynamics near heteroclinic networks*, Physica D 268 (2014) 34–49.
- [30] A.A.P. Rodrigues, I.S. Labouriau, M.A.D. Aguiar. *Chaotic double cycling*, Dyn. Sys. Int. J. 26(2) (2011) 199–233.

- [31] A.A.P. Rodrigues. *Unfolding a Bykov attractor: from an attracting torus to strange attractors*, Journal of Dynamics and Differential Equations, Accepted pending minor revisions, 2019.
- [32] G. Schwarz. *Lifting smooth homotopies of orbit spaces*, Publications Mathématiques de l’IHÉS, 51 (1980) 37-135.
- [33] A. Wolf, J.B. Swift, H.L. Swinney, J.A. Vastano. *Determining Lyapunov exponents from a time series*, Physica D 16 (1985) 285–317.
- [34] K. Yagasaki. *Melnikov’s method and codimension-two bifurcations in forced oscillations*, J. Differential Equations, 185 (2002) 1–24.

APPENDIX A. GLOSSARY

For $\varepsilon > 0$ small enough, consider the two-parameter family of C^3 -smooth autonomous differential equations

$$\dot{x} = f_{(\tau_1, \tau_2)}(x) \quad x \in \mathbb{S}^3 \quad \tau_1, \tau_2 \in [0, \varepsilon] \quad (\text{A.1})$$

where \mathbb{S}^3 denotes the unit sphere, endowed with the usual topology. Denote by $\varphi_{(\tau_1, \tau_2)}(t, x)$, $t \in \mathbb{R}$, the associated flow.

A.1. Attracting set. A subset Ω of a topological space \mathcal{M} for which there exists a neighborhood $U \subset \mathcal{M}$ satisfying $\varphi(t, U) \subset U$ for all $t \geq 0$ and $\bigcap_{t \in \mathbb{R}^+} \varphi(t, U) = \Omega$ is called an *attracting set* by the flow φ , not necessarily connected. Its basin of attraction, denoted by $\mathbf{B}(\Omega)$ is the set of points in \mathcal{M} whose orbits have ω -limit in Ω . We say that Ω is *asymptotically stable* (or that Ω is a *global attractor*) if $\mathbf{B}(\Omega) = \mathbb{S}^3 \setminus \{\mathbf{O}\}$. An attracting set is said to be *quasi-stochastic* if it encloses periodic solutions with different Morse indices, structurally unstable cycles, sinks and saddle-type invariant sets.

A.2. Heteroclinic phenomenon and Bykov cycle. Suppose that O_1 and O_2 are two hyperbolic saddle-foci of (A.1) with different Morse indices (dimension of the unstable manifold). There is a *heteroclinic cycle* associated to O_1 and O_2 if $W^u(O_1) \cap W^s(O_2) \neq \emptyset$ and $W^u(O_2) \cap W^s(O_1) \neq \emptyset$. For $i, j \in \{1, 2\}$, the non-empty intersection of $W^u(O_i)$ with $W^s(O_j)$ is called a *heteroclinic connection* between O_i and O_j , and will be denoted by $[O_i \rightarrow O_j]$. Although heteroclinic cycles involving equilibria are not a generic feature within differential equations, they may be structurally stable within families of systems which are equivariant under the action of a compact Lie group $\mathcal{G} \subset \mathbb{O}(n)$, due to the existence of flow-invariant subspaces [15].

A heteroclinic cycle between two hyperbolic saddle-foci of different Morse indices, where one of the connections is transverse (and so stable under small perturbations) while the other is structurally unstable, is called a Bykov cycle. A *Bykov network* is a connected union of heteroclinic cycles, not necessarily in finite number. We refer to [19] for an overview of heteroclinic bifurcations and substantial information on the dynamics near different kinds of heteroclinic cycles and networks.

A.3. Chirality. Given a Bykov cycle, there are two different possibilities for the geometry of the flow around Γ , depending on the direction trajectories turn around the one-dimensional heteroclinic connection from O_1 to O_2 . To make this rigorous, we need the following concepts adapted from [23].

Let V_1 and V_2 be small disjoint neighbourhoods of O_1 and O_2 with disjoint boundaries ∂V_1 and ∂V_2 , respectively. Trajectories starting at ∂V_1 near $W^s(O_1)$ go into the interior of V_1 in positive time, then follow the connection from O_1 to O_2 , go inside V_2 , and then come out at ∂V_2 . Let \mathcal{Q} be a piece of trajectory like this from ∂V_1 to ∂V_2 . Now join its starting point to

its end point by a line segment, forming a closed curve, that we call the *loop* of \mathcal{Q} . The loop of \mathcal{Q} and the cycle Γ are disjoint closed sets.

We say that the two saddle-foci O_1 and O_2 in Γ have the same *chirality* if the loop of every trajectory is linked to Γ in the sense that the two closed sets cannot be disconnected by an isotopy. Otherwise, we say that O_1 and O_2 have different chirality.

A.4. Saturated horseshoe. Given $(\tau_1, \tau_2) \in [0, \varepsilon]^2$, suppose that there is a cross-section \mathcal{S}_λ to the flow $\varphi_{(\tau_1, \tau_2)}$ such that $\mathcal{S}_{(\tau_1, \tau_2)}$ contains a compact set $\mathcal{K}_{(\tau_1, \tau_2)}$ invariant by the first return map $\mathcal{F}_{(\tau_1, \tau_2)}$ to $\mathcal{S}_{(\tau_1, \tau_2)}$. Assume also that $\mathcal{F}_{(\tau_1, \tau_2)}$ restricted to $\mathcal{K}_{(\tau_1, \tau_2)}$ is conjugate to a full shift on a finite alphabet. Then the *saturated horseshoe associated to $\mathcal{K}_{(\tau_1, \tau_2)}$* is the flow-invariant set

$$\widetilde{\mathcal{K}_{(\tau_1, \tau_2)}} = \{\varphi_{(\tau_1, \tau_2)}(t, x) : t \in \mathbb{R}, x \in \mathcal{K}_{(\tau_1, \tau_2)}\}.$$

A.5. Rotational horseshoe. Let \mathcal{H} stand for the infinite annulus $\mathcal{H} = \mathbb{S}^1 \times \mathbb{R}$. We denote by $\text{Homeo}^+(\mathcal{H})$ the set of homeomorphisms of the annulus which preserve orientation. Given a homeomorphism $f : X \rightarrow X$ and a partition of $m > 1$ elements R_0, \dots, R_m of X , the itinerary function $\xi : X \rightarrow \{0, \dots, m-1\}^{\mathbb{Z}} = \Sigma_m$ is defined by $\xi(x)(j) = k$ if and only if $f^j(x) \in R_k$ for every $j \in \mathbb{Z}$. Following [26], we say that a compact invariant set $\Lambda \subset \mathcal{H}$ of $f \in \text{Homeo}^+(\mathcal{H})$ is a rotational horseshoe if it admits a finite partition $P = \{R_0, \dots, R_{m-1}\}$ with R_i open sets of Λ so that

- (1) the itinerary ξ defines a semi-conjugacy between $f|_\Lambda$ and the full-shift $\sigma : \Sigma_m \rightarrow \Sigma_m$, that is $\xi \circ f = \sigma \circ \xi$ with ξ continuous and onto;
- (2) for any lift F of f , there exist a positive constant k and m vectors $v_0, \dots, v_{m-1} \in \mathbb{Z} \times \{0\}$ so that:

$$\left\| (F^n(x) - x) - \sum_{i=0}^{n-1} v_{\xi(x)(i)} \right\| < k \quad \text{for every } x \in \pi^{-1}(\Lambda), \quad n \in \mathbb{N}.$$

A.6. SRB measure. Given an attracting set Ω for a continuous map $R : \mathcal{M} \rightarrow \mathcal{M}$ of a compact manifold \mathcal{M} , consider the Birkhoff average with respect to the continuous function $T : \mathcal{M} \rightarrow \mathbb{R}$ on the R -orbit starting at $x \in \mathcal{M}$:

$$L(T, x) = \lim_{n \in \mathbb{N}} \frac{1}{n} \sum_{i=0}^{n-1} T \circ R^i(x). \quad (\text{A.2})$$

Suppose that, for Lebesgue almost all points $x \in \mathbf{B}(\Omega)$, the limit (A.2) exists and is independent on x . Then L is a continuous linear functional in the set of continuous maps from \mathcal{M} to \mathbb{R} (denoted by $C(\mathcal{M}, \mathbb{R})$). By the Riesz Representation Theorem, it defines a unique probability measure μ such that:

$$\lim_{n \in \mathbb{N}} \frac{1}{n} \sum_{i=0}^{n-1} T \circ R^i(x) = \int_{\Omega} T d\mu \quad (\text{A.3})$$

for all $T \in C(\mathcal{M}, \mathbb{R})$ and for Lebesgue almost all points $x \in \mathbf{B}(\Omega)$. If there exists an ergodic measure μ supported in Ω such that (A.3) is satisfied for all continuous maps $T \in C(\mathcal{M}, \mathbb{R})$ for Lebesgue almost all points $x \in \mathbf{B}(\Omega)$, where $\mathbf{B}(\Omega)$ has positive Lebesgue measure, then μ is called a SRB measure and Ω is a SRB attractor.

A.7. Symmetry and lifting by rotation. Given a group \mathcal{G} of endomorphisms of \mathbb{S}^3 , we will consider two-parameter families of vector fields $(f_{(\tau_1, \tau_2)})$ under the equivariance assumption

$$f_{(\tau_1, \tau_2)}(\gamma x) = \gamma f_{(\tau_1, \tau_2)}(x)$$

for all $x \in \mathbb{S}^3$, $\gamma \in \mathcal{G}$ and $(\tau_1, \tau_2) \in [0, \varepsilon]^2$. For an isotropy subgroup $\tilde{\mathcal{G}} < \mathcal{G}$, we will write $\text{Fix}(\tilde{\mathcal{G}})$ for the vector subspace of points that are fixed by the elements of $\tilde{\mathcal{G}}$. Observe that, for \mathcal{G} -equivariant differential equations, the subspace $\text{Fix}(\tilde{\mathcal{G}})$ is flow-invariant.

The authors of [7, 30] investigate how some properties of a \mathbb{Z}_2 -equivariant vector field on \mathbb{R}^n lift by a rotation to properties of a corresponding vector field on \mathbb{R}^{n+1} . For the sake of completeness, we review some of these properties.

Let f_n be a $\mathbb{Z}_2(\gamma_n)$ -equivariant vector field on \mathbb{R}^n . Without loss of generality, we may assume that f_n is equivariant by the action of

$$\gamma_n(x_1, x_2, \dots, x_{n-1}, y) = (x_1, x_2, \dots, x_{n-1}, -y).$$

The vector field f_{n+1} on \mathbb{R}^{n+1} is obtained by adding the auxiliary equation $\dot{\theta} = \omega > 0$ and interpreting (y, θ) as polar coordinates. In cartesian coordinates $(x_1, \dots, x_{n-1}, r_1, r_2) \in \mathbb{R}^{n+1}$, this equation corresponds to the system $r_1 = |y| \cos \theta$ and $r_2 = |y| \sin \theta$. The resulting vector field f_{n+1} on \mathbb{R}^{n+1} is called the *lift by rotation of f_n* , and is $\text{SO}(2)$ -equivariant in the last two coordinates.

Given a set $\Lambda \subset \mathbb{R}^n$, let $\mathcal{L}(\Lambda) \subset \mathbb{R}^{n+1}$ be the lift by rotation of Λ , that is,

$$\left\{ (x_1, \dots, x_{n-1}, r_1, r_2) \in \mathbb{R}^{n+1} : (x_1, \dots, x_{n-1}, |(r_1, r_2)|) \text{ or } (x_1, \dots, x_{n-1}, -|(r_1, r_2)|) \in \Lambda \right\}.$$

It was shown in [7, Section 3] that, if f_n is a $\mathbb{Z}_2(\gamma_n)$ -equivariant vector field in \mathbb{R}^n and f_{n+1} is its lift by rotation to \mathbb{R}^{n+1} , then:

- (1) If p is a hyperbolic equilibrium of f_n outside $\text{Fix}(\mathbb{Z}_2(\gamma_n))$, then $\mathcal{L}(\{p\})$ is a hyperbolic periodic solution of f_{n+1} with minimal period $2\pi/\omega$.
- (2) If p is a hyperbolic equilibrium of f_n lying in $\text{Fix}(\mathbb{Z}_2(\gamma_n))$, then $\mathcal{L}(\{p\})$ is a hyperbolic equilibrium of f_{n+1} .
- (3) If $[p_1 \rightarrow p_2]$ is a k -dimensional heteroclinic connection between equilibria p_1 and p_2 and it is not contained in $\text{Fix}(\mathbb{Z}_2(\gamma_n))$, then it lifts to a $(k+1)$ -dimensional connection between the periodic orbits $\mathcal{L}(\{p_1\})$ and $\mathcal{L}(\{p_2\})$ of f_{n+1} .
- (4) If Λ is a compact f_n -invariant asymptotically stable set, then $\mathcal{L}(\Lambda)$ is a compact f_{n+1} -invariant asymptotically stable set.

(L. Castro) CENTER FOR HEALTH TECHNOLOGY AND SERVICES RESEARCH - CINTESIS, UNIVERSITY OF PORTO, RUA DR. PLÁCIDO DA COSTA, 4200-450 PORTO, PORTUGAL

E-mail address, L. Castro: luisacastr@med.up.pt

(A. A. P. Rodrigues) CENTRO DE MATEMÁTICA DA UNIVERSIDADE DO PORTO, AND FACULDADE DE CIÊNCIAS DA UNIVERSIDADE DO PORTO, RUA DO CAMPO ALEGRE 687, 4169-007 PORTO, PORTUGAL

E-mail address, A.A.P.Rodrigues: alexandre.rodrigues@fc.up.pt